Left Ventricular Heart Phantom for Wall Motion Analysis

Kerstin Müller[1,2], Andreas K. Maier[1,2], Peter Fischer[1,2], Bastian Bier[1], Günter Lauritsch[3], Chris Schwemmer[1,2], Rebecca Fahrig[4] and Joachim Hornegger[1,2]

[1] *Pattern Recognition Lab, Department of Computer Science, Friedrich-Alexander Universität Erlangen-Nürnberg, Erlangen, Germany*
[2] *Erlangen Graduate School in Advanced Optical Technologies (SAOT), Friedrich-Alexander Universität Erlangen-Nürnberg, Erlangen, Germany*
[3] *Siemens AG, Healthcare Sector, Forchheim, Germany*
[4] *Department of Radiology, Stanford University, Stanford, CA, USA*

Introduction

With the technology of C-arm CT it is possible to gain intraprocedural anatomical and functional information of the cardiac chambers [1].

➢ Consideration of motion is complex and severely ill-posed. Sophisticated techniques of motion estimation and compensation are needed.

Goal: Provide publicly available realistic heart ventricle datasets with different motion patterns and contraction behavior for evaluation.

Left Ventricular Heart Phantom Generation

1. Acquisition Parameters

   - Cardiac protocol with ~5 s and 133 projection images covering 200°, 30 fps and isotropic resolution of 0.31 mm/pixel (0.2 mm in isocenter).

     ➢ Real acquisition scenario and geometry calibration from a clinical angiographic C-arm system.

2. XCAT-based Phantom Datasets [2]

   - Monochromatic: same absorption as water with different densities[1]
     left ventricle bloodpool density: 2.5 g/cm^3 (1500 HU)
     myocardial wall density: 1.5 g/cm^3 (500 HU)
     blood of aorta: 2.0 g/cm^3 (1000 HU)
   - Polychromatic: bone, bone marrow and (if present) the catheter have attenuation values according to NIST Table[2], other structures have absorption characteristic like water.

3. Surface Mesh Generation

   - The analytic 4-D spline model describing the left ventricle can be sampled at any number of points (here: 2500) for every acquisition time point [3].

4. Modelling Pathologic Motion Patterns

   - For every normalized time point $t \in [0,1]$ for the whole scan, exists a 2-D spline surface $\boldsymbol{s} \in [0,1]^2$.
   - Set $\mathcal{C}$ of cubic B-spline control points $\boldsymbol{c} \in \mathbb{R}^2$, the motion defect is defined inside bounding box $\mathcal{B}$ with defect control points in $\mathcal{C}_{path}$.
   - Smooth transition between $\mathcal{B}$ and the healthy tissue: flexibility parameter σ (larger σ, smoother transition).
   - Tessellation procedure $T(\boldsymbol{s},t): \mathbb{R}^2 \rightarrow \mathbb{R}^3$, points on 2-D spline surface $\boldsymbol{s} \in [0,1]^2$ are assigned to a 3-D coordinate $\boldsymbol{x}(t) = T(\boldsymbol{s},t)$ for each time point t.
   - Two kinds of motion defect: akinetic and dyskinetic motion. Motion defect control by phase shift parameter $\delta \in [0,1]$.
   - Deformed 3-D coordinate:

$$\begin{aligned} \boldsymbol{x}_{path}(t) &= (1 - w(\boldsymbol{s},t)) \cdot T(\boldsymbol{s},t) + w(\boldsymbol{s},t) \cdot T(\boldsymbol{s},t-\delta), \\ w(\boldsymbol{s},t) &= \frac{\sum_{\boldsymbol{c} \in \mathcal{C}_{path}} w'(\boldsymbol{s},\boldsymbol{c},t)}{\sum_{\boldsymbol{c} \in \mathcal{C}} w'(\boldsymbol{s},\boldsymbol{c},t)}, \\ w'(\boldsymbol{s},\boldsymbol{c},t) &= e^{-\frac{1}{2\sigma^2}||\boldsymbol{s}-\boldsymbol{c}||_2^2}. \end{aligned}$$

   - The radial basis function $w'(\boldsymbol{s},\boldsymbol{c},t)$ gives a small weight to control points far away from the current spline surface point $\boldsymbol{s}$ and a higher weight to close control points.
   - Akinetic (no motion) is realized by setting $\delta = t - t_0$, here: $t_0 = 0$.

Contact
✉ kerstin.mueller@cs.fau.de
http://www5.cs.fau.de/~mueller

The authors gratefully acknowledge funding support from the NIH grant R01 HL087917 and by Siemens AG, Healthcare Sector and of the Erlangen Graduate School in Advanced Optical Technologies (SAOT) by the German Research Foundation (DFG) in the framework of the German excellence initiative.

Datasets

Six different phantom datasets (mono-/polychromatic, raw and preprocessed data, surface meshes and geometry)

- static heartphase of 75% (p_0)
- dynamic 60 bpm, normal contraction (p_1)
- dynamic 60 bpm, lateral phase shift of δ = 20% (p_2)
- dynamic 60 bpm, lateral phase shift of δ = 30% (p_3)
- dynamic 60 bpm, lateral wall defect (p_4)
- dynamic 60 bpm, normal contraction with catheter (p_5)

➢ Available online at https://*conrad.stanford.edu/data/heart*

Dataset	Motion Defect	HR [bpm]	Ejection Fraction (EF) [%] [4]	Systolic Dyssynchrony Index (SDI) [%] [5]
p_0	none	n.a.	n.a.	n.a.
p_1	none	60	62.37	4.16
p_2	20% [lateral]	60	60.40	6.47
p_3	30% [lateral]	60	53.67	12.74
p_4	defect lateral	60	38.70	5.05
p_5	none	60	62.37	4.16

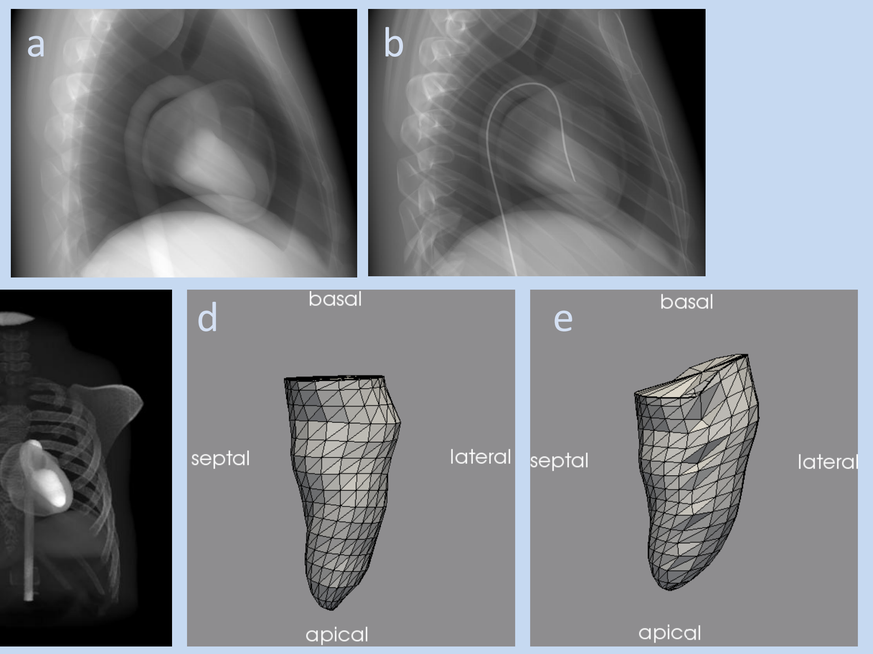

Figure 1: Example images of the available phantom datasets. (a) Simulated 2-D projection image, with contrasted left ventricle, myocardium and aorta. (b) Simulated 2-D projection image with catheter. (c) Anterior view of the generated phantom dataset. (d) Generated triangle mesh of the left ventricle with normal contraction and (e) of the left ventricle with wall defect.

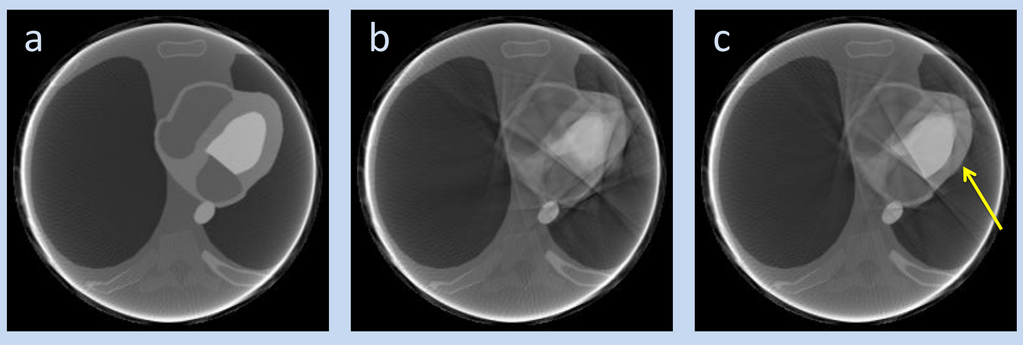

Figure 2: Example reconstructions of three available phantom datasets with the monochromatic projections. (a) Standard FDK reconstruction of the static phantom and a relative heart phase of 75%. (b) Standard FDK reconstruction of the phantom with normal contraction ability and 60 bpm and (c) an introduced lateral wall defect.

References

[1] Müller et al., "Evaluation of interpolation methods for surface-based motion compensated tomographic reconstruction for cardiac angiographic C-arm data," Med Phys, vol. 40, no. 3, 2013.
[2] Segars et al., "A realistic spline-based dynamic heart phantom," IEEE TNS, vol. 46, no. 3, 1999.
[3] Maier et al., "Fast simulation of X-ray projections of spline-based surfaces using an append buffer," Phys Med Biol, vol. 57, no. 19, 2012.
[4] Pfisterer et al., "Range of normal values for left and right ventricular ejection fraction at rest and during exercise assessed by radionuclide angiocardiography," Eur Heart J, vol. 6, no. 8, 1985.
[5] Kapetanakis et al., "Real-time three-dimensional echocardiography a novel technique to quantify global left ventricular mechanical dyssynchrony," Circulation, vol. 112, no. 7, 2005.
[1] http://www.imp.uni-erlangen.de/forbild
[2] http://physics.nist.gov/PhysRefData/Xcom/html/xcom1.html